Journal of the Optical Society of Korea, Vol. 8, No. 4, December 2004, pp. 174-181

Optical System Design for Thermal Target Recognition by Spiral Scanning [TRSS]

Jai-Soon Kim*, Jin-Kyung Yoon, Ho-Chan Lee, and Jai-Hyung Lee
School of Physics, Seoul National University, Seoul 151-747, KOREA

Hye-Kyung Kim
EOsystem.co., Ltd., Incheon 404-250, KOREA

Seung-Churl Lee and Keun-Ok Ahn
Agency for Defense Development, Daejeon 305-600, KOREA

(Received October 20, 2004)

Various kinds of systems, that can do target recognition and position detection simultaneously by using infrared sensing detectors, have been developed. In this paper, the detection system TRSS (Thermal target Recognition by Spiral Scanning) adopts linear array shaped uncooled IR detector and uses spiral type fast scanning method for relative position detection of target objects, which radiate an IR region wavelength spectrum. It can detect thermal energy radiating from a 9 m-size target object as far as 200 m distance. And the maximum field of a detector is fully filled with the same size of target object at the minimum approaching distance 50 m. We investigate two types of lens systems. One is a singlet lens and the other is a doublet lens system. Every system includes one aspheric surface and free positioned aperture stop. Many designs of F/1.5 system with $\pm 5.2°$ field at the Efl=20, 30 mm conditions for single element and double elements lens system respectively are compared in their resolution performance [MTF] according to the aspheric surface and stop position changing on their optimization process. Optimum design is established including mechanical boundary conditions and manufacturing considerations.

OCIS codes : 080.0080, 110.3080, 120.1880, 130.3060, 220.0220

I. INTRODUCTION

Many kinds of detection and recognition systems for IR radiation information have been developed since the 1930's. The intelligence uses of thermal imaging systems include target acquisition, action control, aerial navigation, surveillance and information gathering [1]. In the early years, various scanning methods have been developed to achieve a proper size IR image with small numbers of detector elements, but single frame large images are recently available [1-5]. And so, the scanning methods are used for another purpose of special application systems. We consider a special system need to have target recognition along with action and treatment functions also, as an example of diagram in Fig. 1. Before doing a proper action to the target, the system needs to know what (recognition) and where (location) the target is. To accomplish the dual-purpose functions, some systems are equipped with gyros for checking absolute coordinates and some have used a two-dimensional array detector for image capture and processing. In this paper, target detection of an actual total system is performed in 3 kinds of different

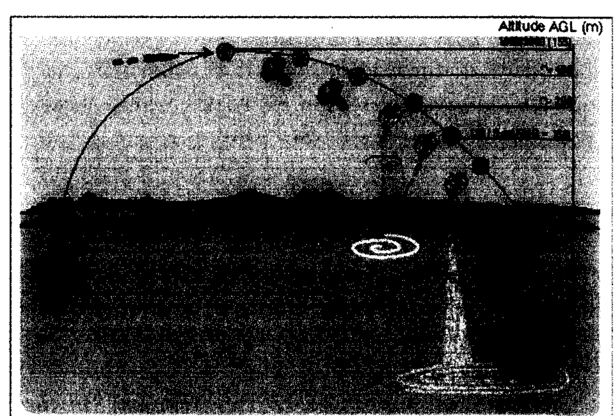

FIG. 1. Layout of the target detect/act system.

channel detecting systems. Passive microwave, active microwave and IR detection systems take different roles for the correct shape and position recognition of the target object. Intelligent hybrid analysis cooperatively gets the exactly correct decision for the proper treatment (attacking, et cetera...) to the recognized target object.

In this paper we mainly concentrate on the role of an optical system (Thermal target Recognition by Spiral Scanning: TRSS) and its design. The recognition methodologies of IR detection systems, including imaging and non-imaging, mainly depend on the types of detectors that can be developed at the time. Historical review of IR systems and detectors almost for 1 century is shown in Table 1 [3,4,6].

To set up an IR system profitable for detecting, we check the usable spectrum band, optical material and detector for balancing that bandwidth. We use 8~12 μm wavelength range among the general mid and far spectrum ranges for thermal detection in an air based environment according to the absorption by the atmospheric window [4]. There are many kinds of commercial materials that have good transmittance for all of those spectrum ranges and mechanical characteristics [4]. Among them, Germanium has higher refractive index that can serve better for optical designing, while the Silicon shows more resistance to gravitational shock and vibration. The detector is an important factor for processing the detected signal, and we select a bolometer type uncooled linear array detector as a thermal effect transducer for the TRSS system [3-5].

Optical materials for the IR spectrum range are expensive and the unwanted diffraction noise and scattering effect are relatively smaller than for shorter wavelength light. Applications of aspheric and diffraction surfaces on the IR lens are investigated relatively earlier than for visible range optics [7-9]. In this paper we apply one aspherical surface for both single and double lens system. The proper thickness and surface treatment (antireflection and hardness coating) for IR material (Germanium) are considered together [4,6,7].

II. SYSTEM REQUIREMENTS

A TRSS system hanging on a parachute has a viewing field rotating with the conic trajectory while falling down to the ground. So the full-size viewing field of the TRSS on the ground is filled with an instantaneous small field by spiral shaped scanning as shown in Fig. 2. To fulfill the system requirements we consider several important factors as follows. Warhead ranges, descent rate, hang angle and scan rates per second etc. are specified quantitatively by analyzing physical factors. Field angle of the optical system should be small enough that it can recognize the direction of the proper size thermal target by checking its angular position on the conic trajectory. The scanning optical system tilting to the off axis with some appropriate angle is rotating in order to draw a spiral-shape-scanned field trajectory on the ground. One circular field drawn by the first spiral turn (at the maximum starting altitude) of narrow sighting (small instantaneous field of view) TRSS decides the maximum field boundary of the recognition mission and then, the next inside turns should not lose any small fraction of the inside field area information. An instantaneous field of a previous turn must be overlapped with the field of next turn, in order to keep full field recognition.

The motion of a TRSS system is decided by two factors, one is gravitational falling and the other is the wind effect. Falling is in the vertical direction only but wind can blow in any direction including horizontal. One periodic turn of the TRSS system attached at the bottom of the descending apparatus is shown in Fig. 3. The time interval between two modular TRSS in this figure is just one spiral revolution. Here, H is a vertical drop distance which depends on the gravity and wind direction, and its ranges are 10~20 m/sec in our system. D is a horizontal drift by wind and it decides stability of the system against the weather. W is a one-dimensional static full field of the TRSS

TABLE 1. IR Detector and Scanning Methods.

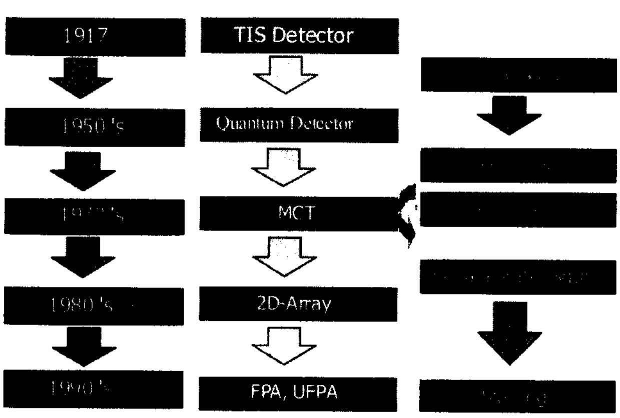

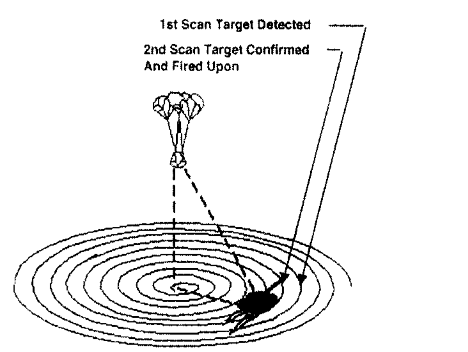

FIG. 2. Falling down of a TRSS.

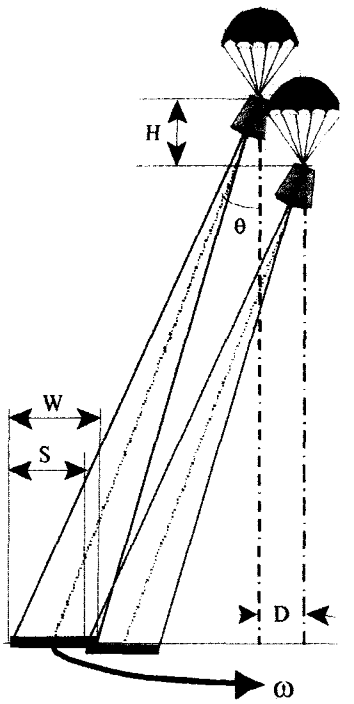

FIG. 3. Field overlap of one periodic turn of the TRSS.

system in the radial direction (in order to make a correct recognition of the direction factor, it should be as small as possible but at least, larger than the minimum size of a target object). In the case of a large vehicle (tank, etc.) W extends 9 m around. W must be larger than the total shifting distance S even in the worst case (drift by wind acts in the same direction as the shift by gravitational falling). The horizontal shifting distance S is decided by inward movement of the instantaneous field according to the spiral trajectory that is caused by the vertical drop velocity V_V and horizontal component of blowing wind velocity V_H multiplied by iteration time 1/n sec. The requirement of the system is that the scanning field of successive turn in any situation should overlap with the previous turn. So, the dynamic equation for field overlap condition is as follows.

$$W \geq S = H \cdot \tan\theta + D$$
$$= \frac{1}{n} \cdot (V_V \cdot \tan\theta + V_H) \quad (1)$$

Here, n is the number of revolutions per unit time (second). So, 1/n sec is the iteration time. And Θ is the tilt angle of an optics module relative to the vertical descent direction.

The velocity V_V depends on the gravitational fall of the transferring equipment (parachute or other) and the climate of the application region. General limiting velocity of 20 m/sec is obtained from experimental data. In the case of applying 30-degrees tilt angle and 10 revolutions per one second, the system can resist against up to 78 m/s horizontal wind velocity. So, it has remarkable stability against the environmental alterations.

III. LENS DESIGN

1. Design Condition / System Specification

Transmission wavelength regions of the IR spectrum in air are 3~5 μm and 8~12 μm [4]. The TRSS system uses bandwidth of 8~12 μm range (long IR region) that is related to the detector characteristics and material considerations [2,3,7]. The combinations of a focal length and a field angle decide the diagonal length of a detector array (commercial 50 μm pixel size 2 dimensional array detector for the prototype testing and custom designed hi-resolution of 20 μm pixel size linear detector for the optimum system are considered). Modulation transfer function (MTF) property of the optical system at the maximum target spatial resolution should meet the appropriate system requirement according to the one-pixel size of the detector in use. Alteration of the field angle according to the variation of the detection height is shown in Fig. 4 (a). Vertical spatial resolution normal to the scanning direction is related to the one-pixel size of the detector array and to the effective focal length. Horizontal spatial resolution is decided by scanning velocity, detection height and effective cycle of the pixel clock.

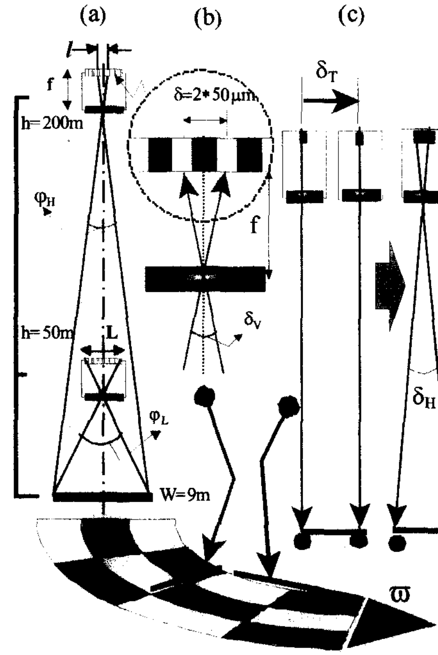

FIG. 4. (a) Field angles, (b) Vertical spatial resolution, (c) Horizontal spatial resolution.

Fig. 4 (b) & (c) are diagrams for both spatial resolutions.

Detection height h, focal length of the TRSS and the size of a detector L decide effective observation field angles (from high altitude φ_H to low altitude φ_L). The minimum object size W captured in nearest observation should be larger than the proper target size being considered.

$$L \geq 2f \cdot \tan\frac{\varphi}{2} = f \cdot \frac{W}{h} \qquad (2)$$

Detector dimension δ (2 pixels) and focal length f inherently decide angular acuity for vertical direction δ_V.

$$\delta_V = \frac{\delta}{f} = \frac{2 \cdot pixelsize}{f} \qquad (3)$$

In the case that the sensing speed of the detector is fixed to ν Hz, angular scanning velocity ω and 2 clock units of a detector δ_T decide angular acuity for horizontal direction δ_H.

$$\delta_H = \omega \cdot \delta_T = \omega \cdot \frac{2}{\nu} \qquad (4)$$

And all the spatial resolutions are obtained by multiplying the observation height by the angular acuity.

The first order parameters for optical design are induced by considering above equations and the results are summarized in Table 2. System parameters are determined on the boundary conditions of W=9 m, h=5~200 m, ω=10 rev/s (62.4 rad/s) and the pixel size of a detector $\delta/2$ is from 50 mm for the low-resolution to 20 mm for the high-resolution system. In processing optimization and analysis, over all lengths (OAL) and maximum lens diameters (MLD) are confined to 60 mm and 20 mm respectively. All optical analyses and optimizations in this paper are performed with Zemax lens design software [10,11].

TABLE 2. System Parameters for TRSS.

Boundary Conditions	W=9 m, h=50~200 m, $\delta/2$ =50~20 μm, ω=10 rev/s	
L	4 mm	6 mm
f	20 mm	30 mm
φ_L	5.2°	
φ_H	1.3°	
δ_V	Minimum 5 mrad/pair 200 lp/rad	Maximum 0.833 mrad/pair 1200 lp/rad
$\nu = 1/\delta_H (= \delta_V)$	faster than 50 kHz	
F/#	1.5	
Size	MLD 20 mm, OAL 60 mm	

2. Single Lens Design.

Spherical single lens design is investigated as a base point for the single aspheric lens system. Starting lens shape is decided by the best form bending [12]. To satisfy small coma and minimum longitudinal spherical aberration (LA or SA) condition for a single thin element, the lens should be represented as follows.

$$LA_p' = LA_p\left(\frac{l'}{l}\right)^2 - y^2 l'^2 \sum(Gsum) \qquad (5)$$

Here, the characters with a prime (') occur in image space and without prime occur in objective space, p means primary (3^{rd} order approximation). Object and image distance are designated as l' and l respectively, axial ray height on the lens surface is y. *Gsum* in the parenthesis refers to the following 6 equations.

$$G_1 = \frac{1}{2}n^2(n-1), \quad G_2 = \frac{1}{2}(2n+1)(n-1), \quad G_3 = \frac{1}{2}(3n+1)(n-1),$$
$$G_4 = \frac{1}{2}(n+2)(n-1)/n, \quad G_5 = 2(n-1)^2/n, \quad G_6 = \frac{1}{2}(3n+2)(n-1)/n, \qquad (6)$$

Minimum LA can be found by differentiating Eq (5) with respect to c_1 (c_j is a curvature of the j surface).

When the objective is infinite, form factors and focus factors are decided as follows.

$$\frac{c_1}{c_2} = \frac{n(2n+1)}{(2n^2 - n - 4)} = \frac{R_2}{R_1} \quad ; \text{ When the object is infinite} \qquad (7)$$

$$\frac{1}{f} = (n-1)\cdot(c_1 - c_2) = (n-1)\cdot\left(\frac{1}{R_1} - \frac{1}{R_2}\right) \qquad (8)$$

In the case of n=4 and f=20 mm, R_1 and R_2 values at the thin lens approximation are 20 mm and 30 mm respectively.

However, in real thick lens calculations R-values are affected by Germanium lens thickness. The shape and data for starting point of the single element lens design are presented in Fig. 5. Some boundary conditions are added on the first order specific conditions that are described in Table 2. Air gap thickness between the

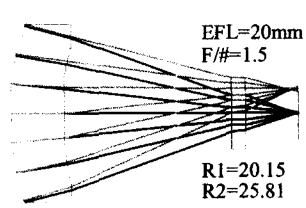

FIG. 5. Best-form Lens.

last lens surface and the front surface of the 1 mm-thickness germanium window is longer than 2 mm (because of mechanical parts dimension and assembling) and the vacuum gap between the rear surface of that window and the detector surface is fixed to 4 mm in optimization.

A. Single Spherical Lens. (SS)

At first, after applying stop shift in optimization, optical performances of each lens are checked with resolution (MTF at 10 lp/mm) graphs [2,12]. In this case, the minimum MTF values are selected out of all the applied sagittal and tangential fields after finding the best defocus position. OAL, MLD and the thickness of each layer are considered as a boundary condition for the manufacturing factors. In case of the stop positioned left and right sides of the lens element, we simply expect meniscus type landscape lens, which has tolerable residual SA but achieves low field curvature [2,12]. However, the local optimum design shape at each stop position depends on the tradeoff of a numerical aperture (NA) value and the maximum field size. OAL, MLD and MTF graphs according to the stop position variation are shown in Fig. 6. Stop position 0- and 0+ on the x coordinate represent stop at left and right lens surface respectively, and numbers are distances between the stop and the nearest lens surfaces. The single spherical system shows best MTF (over 50% at 10 lp/mm) at -25 mm left stop landscape lens. It can be applied to the array detector that is assembled with element pixel size of 50 μm. MLD is minimum at stop on lens surface status and smaller than 20 mm.

B. Single Lens with one Aspheric Surface. (SA)

Aspheric lenses are designed from the base point of each spherical design. Performance improvements by changing the shape of lens surface from sphere to aspheric surface for the first surface and second surface of a single lens element are compared separately at the same steps of the stop position as the previous single spherical analysis. Two different aspheric surface designations of first and second surface show almost the same optical performances, and the characteristics of the optical quality for the first surface aspheric system are shown in Fig. 7. In here MTF graph is checked at 20 lp/mm and it corresponds to 25 μm element pixel size detector. Different from the SS system, we get two types of good SA systems that show almost same MTF quality. One is long left positioned stop and the other is short right positioned stop system.

3. Double Lens Design

Two types of basic designs are considered as the starting points. One is a periscopic lens and the other is a Petzval type lens [6,12,13]. The periscopic lens that is constituted with two identical landscape lenses and symmetrically aligned between central stop, appears free of distortion, coma and lateral color. It has relatively good performance for low NA and large field system. Preliminary set up is decided by using curvature and distance pick up [10] and optimized at the condition of efl=30 mm and OAL=40 mm. Petzval type is characterized as combining 2f and f focal length lens left f/2 distance between them. It is good for relatively high

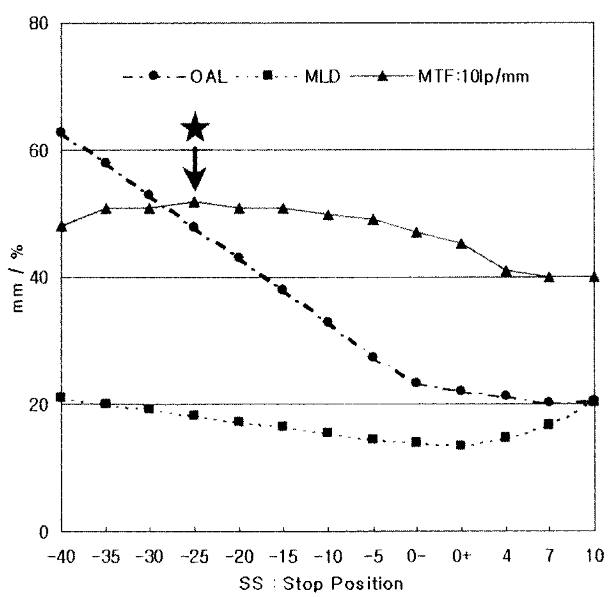

FIG. 6. Optical properties of the single spherical lens.

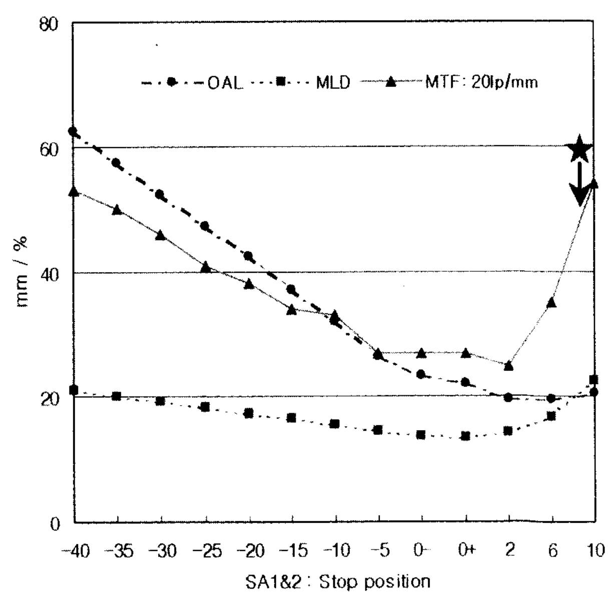

FIG. 7. Optical properties of the single lens with one aspheric surface.

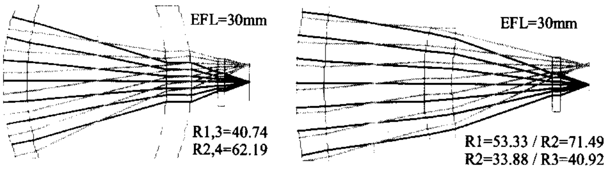

FIG. 8. Periscopic and Petzval type basic doublet design.

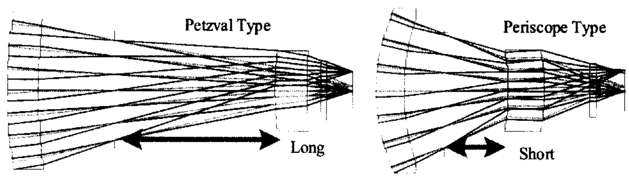

FIG. 9. Long Petzval and short Periscope type lens according to the different stop position.

NA and small field system. Layout and design data for two different types of double spherical elements lens system are shown in Fig. 8. Boundary conditions and 1st order specific conditions are the same as previous single lens system listed in Table 2.

A. Double Spherical Lens. (DS)

From the two different types of basic doublet spherical design data, the aperture stop position is changed gradually from the left side of 1st lens, between two lenses and to the right side of 2nd lens area and the performances are checked with MTF graphs at 20 lp/mm. In case of the center stop position, two types of different stepping are applied separately and the performances are compared. One is the forward stepping from the front surface of a 2nd lens and the other is the backward stepping from the rear surface of the same lens. OAL is confined to the 60 mm maximum and the appropriate resolution condition (20 lp/mm) is selected by showing neighborhood of 50 % MTF values. On condition that the stop move to the left side of a special reference point (positioned at some critical near distance on the left side of the 2nd lens), all the superior designs are shown in Petzval shape. However, when the stop moves to the right side of that reference position, the superior system suddenly turns into the periscope type and it has a short OAL. The representative shapes for the two different types of left stop Petzval

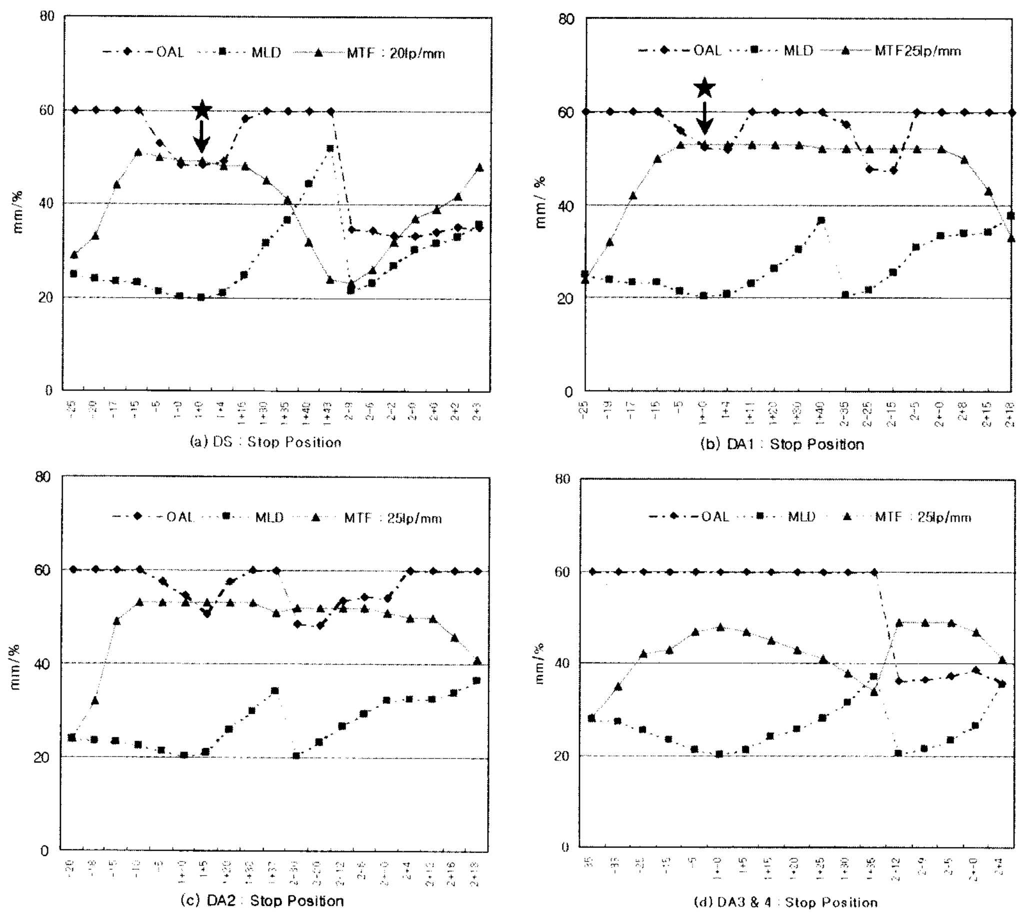

FIG. 10. Optical properties of double lens system. (a) DS : Spherical surfaces, (b) DA1 : 1st surface Aspheric, (c) DA2 : 2nd surface Aspheric, (d) DA3&4 : 3rd or 4th surface Aspheric

type and right stop periscope type systems are shown in Fig. 9. The critical position of the reference stop is 9 mm in front of the 2nd lens and it is definitely distinguished in Fig. 10 (a). OAL and MLD decrease but MTF increase steeply from that point. All the design performances are summarized in Fig. 10 (a).

B. Double Lens with one Aspheric Surface. (DA)

Double aspheric (DA) lenses are designed from the base point of each of the double spherical designs that are decided by the previous procedure. Diffraction limited performances at F/#=1.5 are available with DA lens and it coincides with the data points of more than 50 % performance value in 25 lp/mm MTF graph. And, 25 lp/mm resolution corresponds to the 20 μm element pixel size detector. Four different aspheric surface designations of first and second surface at each lens element are available and named DA1, DA2, DA3, and DA4 in the order. All of the DA1 and DA2 designs are Petzval shape and their optical characteristics are shown in Fig. 10 (b) and 10 (c). Position n+-0 on x-coordinate means aperture stop is located at n^{th} lens element, and optical properties according to the different stop position (one is front and the other is rear surface of nth element) have no big difference even if the lens has considerable thickness. Comparison of DA1 and DA2 graph shows almost the same for MTF and DIA, except small OAL differences at the small section of the stop positions that are located just a little distance in advance of the 2nd element. In case of DA3 and DA4, the two systems show almost identical characteristics and it is shown in Fig. 10 (d): DA3&4. The high inclination OAL line that is similar to the DS graph represents the same phenomena of double spherical lens design. Lens shape of the left side located stop is optimized to the Long Petzval type and the right side located stop is optimized to the Short Periscope type. And DA3&4 system shows diffraction limited performance only in the selected part of a stop position (near 1+-0 and 2-9 at Fig. 10 (d).) and so it is inferior to the DA1 or DA2 system that shows diffraction limited performance almost independent of the stop position.

IV. OPTIMUM DESIGN AND RESULTS

From the previous analysis and considering manufacturing factors, four different types of optical designs are compared eventually. Considering the diamond-turning machine process, aspheric convex surfaces are preferable to the concave surfaces [2,7]. OAL of the single lens system is confined to 40 mm and that of the double lens is confined to 60 mm. Single spherical system is applicable for the 50 μm pixel elements detector (10 lp/mm). Double spherical lens and single lens with one aspherical surface are available for 25 μm (20 lp/mm) and double lens with one aspherical surface is for 20 μm (25 lp/mm). Clock units of a detector should be shortened to get the same amount of horizontal resolution enhancement according to the vertical resolution improvement. All of the four optimum designs are summarized in Table 3. The most front surfaces are coated with DLC hardness and the other surfaces are coated with BBAR condition. The assembly and per-

TABLE 3. Optimum lenses data according to the 4 different design conditions.Design information's for the reference ★ points are indicated in the related Figures. Aspherized surfaces are indicated as * marks on the related curvature radius data.

S/D	MTF		MLD	OAL	Reference	Shape	Data (* Aspheric)		
	lp/mm	%	(mm)	(mm)	★		R (mm)	1st	2nd
SS	10	52	18.2	47.9	Fig. 5.	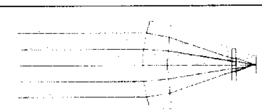	1	29.9	
							2	52.2	
SA	20	49	19.2	19.8	Fig. 6.	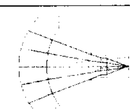	1	13.5*	
							2	12.6	
DS	20	49	20	48.2	Fig. 9 (a).	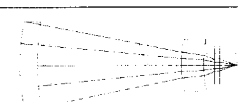	1	43.8	24.8
							2	57.5	30.3
DA	25	52	20.4	52.2	Fig. 9 (b).	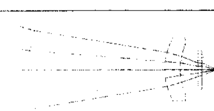	1	26.5*	13.8
							2	26.9	13.2

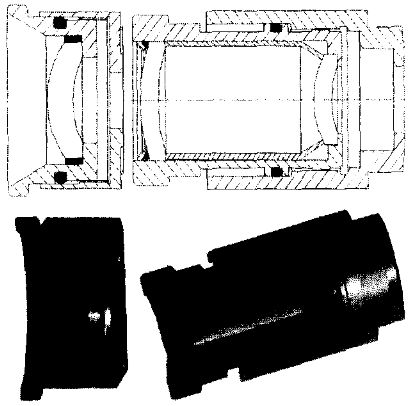

FIG. 11. Assembly and Perspective drawings of SA and DA system.

spective drawings for manufacturing prototype SA and DA systems that include mechanical parts are shown in Fig. 11.

V. CONCLUSION

We examined optical system (TRSS) requirements for detecting shape and position of the target object simultaneously. F/#=1.5, Germanium lens designs of single (efl=20 mm) and double element (efl=30 mm) systems with all spherical and one aspheric surface are investigated. Spherical single lens design is profitable for the 10 lp/mm resolution system, spherical double and one aspheric single lens system is good for 20 lp/mm. One aspheric double lens system shows diffraction limited performance and it fulfils 25 lp/mm resolution. For the future work, manufacturing aspherical surface within some reasonable tolerance ranges and the working out of proper measurement methods for checking optical performance in components and total system will be proceeded. And more design investigations by using the superior detector module, which has a cold shield inside it and is usually adapted to the IR imaging system, are needed [2]. In that case, the cold shield installed beneath a protection window should determine the aperture stop for the total optical system, and so the optical design condition lost the free stop shift ability. Restriction on the much longer back focal length is a big burden for design. Investigation for higher resolution with brighter IR optics system, which has more rigidity in spite of lightweight and compactness, is ongoing research theme for TRSS system.

* Corresponding author : jskim@phya.snu.ac.kr.

REFERENCES

[1] J. M. Lloyd, *Thermal Imaging Systems* (Plenum Press, New York, USA, 1979), pp. 4-16, 283-319.
[2] R. E. Fisher and B. Tadic-Galeb, *Optical System Design* (McGraw-Hill, New York, USA, 2000), pp. 221-233, CHP 7, 8.
[3] I. J. Spiro and M. Schlessinger, *Infrared Technology Fundamentals* (Marcel Dekker, INC. New York, USA, 1989), pp. 151-200.
[4] W. L. Wolfe and G. J. Zissis, *The infrared handbook* (Office of naval research, Department of the Navy, Washington, USA, 1987), CHP 5, 7, 10, 11.
[5] R. R. Shannon and J. C. Wyant, *Applied Optics and Optical Engineering* (Academic Press, New York, USA, 1979) vol. 2, pp. 340-363.
[6] W. J. Smith, *Modern Lens Design* (McGraw-Hill, INC. New York, USA, 1992), CHP 11, 13, 21.
[7] R. Hartmann & W. J. Smith, *Infrared Optical Design and Fabrication* (SPIE, Bellingham, Washington, USA, 1991), pp. 3-18, 164, 184-192, 218.
[8] H. S. Kim, D. H. Lee, H. K. Kim, and G. W. Lee, "Analysis of aspheric and diffraction surface effect for long wavelength infrared lens," Hankook Kwanghak Hoeji, vol. 14, Aug 2003, pp. 369, 376.
[9] H. S. Kim, C. W. Kim, and S. M. Hong, "Design of 4:1 IR zoom afocal telescope," Hankook Kwanghak Hoeji, vol. 9, Jun 1998, pp. 134, 141.
[10] ZEMAX, *Optical Design Program User's Guide* (Focus Software, Incorporated. Tucson, Arizona, USA, 2003).
[11] J. M. Geary, *Introduction to Lens Design* (Willmann-Bell, INC. Virginia, USA, 2002).
[12] R. Kingslake, *Lens Design Fundamental* (Academic Press, INC. Orlando, Florida, USA, 1978), pp. 118-119, 165, 210-217, 251-259.
[13] R. R. Shannon, *The art and science of optical design* (Cambridge university press, New York, USA, 1997), pp. 501, 553-584.